

# Natural limit to the $\gamma$ /hadron separation for a stand alone air Cherenkov telescope

Dorota Sobczyńska

*University of Łódź, Experimental Physics Department, Pomorska 149/153, 90-236  
Łódź, Poland*

---

## Abstract

The  $\gamma$ /hadron separation in the imaging air Cherenkov telescope technique is based on differences between images of a hadronic shower and a  $\gamma$  induced electromagnetic cascade. One may expect for a large telescope that a detection of hadronic events which contains Cherenkov light from one  $\gamma$  subcascade only is possible. In fact, simulations shows that for the MAGIC telescope their fraction in total protonic background is in order of 3.5% to 1% depending on the trigger threshold. It was found out that such images have small sizes (mainly below 400 ph.e.) what corresponds to the sizes of the low energy primary  $\gamma$ 's (below 100 GeV). It is shown that parameters describing a shape of images from one subcascade have similar distributions like a primary  $\gamma$  events, so those parameters are not efficient in all methods of  $\gamma$  selection. Similar studies based on MC simulations are presented also for the images from 2  $\gamma$  subcascade which are products of the same  $\pi^0$  decay.

## *Key words:*

VHE  $\gamma$ -astronomy, Imaging air Cherenkov telescopes,  $\gamma$ /hadron separation

*PACS:* :95.55.Ka;95.55.Vj;95.75-z;95.75.Mn;95.85.Pw;95.85.Ry

---

## 1 Introduction

The first TeV  $\gamma$  source - the Crab Nebula was discovered by the Whipple collaboration in 1989 [1] and it has begun the very fast development of ground-based  $\gamma$  astronomy. It was done by using a 10m-diameter telescope, which collected Cherenkov light produced in the atmosphere by charged fast particles from the shower. The light recorded by a matrix of photomultipliers (camera) mounted in the focal plane producing the light image of the shower. In 1985 Hillas [2]

---

*Email address:* ds@kfd2.phys.uni.lodz.pl (Dorota Sobczyńska).

proposed a method of  $\gamma$  selection from hadronic background, orders of magnitude larger than a signal from a  $\gamma$ -source. Parameters suggested by Hillas describe the shape and the orientation of the image. The direction of the main image axis determines the direction of the primary CR particle, a narrow shape indicates a  $\gamma$  as a primary particle.

Imaging air Cherenkov telescopes (IACT) have been used for years to discover new  $\gamma$  ray sources and determine their fluxes. Larger telescopes are built, stereoscopy is used to lower the energy thresholds and improve the sensitivity, but the main idea of  $\gamma$ /hadron separation remains the same. Major contributions to the development of the ground-based  $\gamma$ -astronomy have recent experiments with very large reflectors like CANGAROO [3], HESS [4], MAGIC [5], VERITAS [6].

On the one hand very large telescopes make detection of low energy events possible, on the other hand it requires parabolical shape of the main reflector dish (like that in MAGIC) to avoid broadening of the Cherenkov light time profile. Unfortunately this kind of telescopes, in spite of Cotton-Devis devices, have non-negligible aberrations - one of the sources of worsening the  $\gamma$  selection. The  $\gamma$ /hadron separation becomes more difficult in the low energy region (below 100 GeV) because of higher relative fluctuations in the shower development, which results in larger fluctuations of the Cherenkov light density and in image parameters.

As expected, telescopes may be triggered by light coming from one charge particle track only, like that of a muon. When the image contains photons from one particle only and the impact parameter is larger than 80 m, then it is very similar to a  $\gamma$  cascade image. Rejecting such background is possible by using fast FADC in the readout system [7] because it has a very narrow arrival time distribution of the Cherenkov photons.

It can happen that all photons in a hadron-initiated shower registered by the telescope are created by one electromagnetic subcascade. From now on I call it 'false  $\gamma$  image'. There is no physical reason for such images to be different from primary  $\gamma$ -induced events. Both should have similar angular and arrival time distributions. Subcascades are created in the showers mostly by  $\pi^0$  decay process. It is also possible that an image contains photons from only two  $\gamma$  subcascades, which are products of the same  $\pi^0$  decay. I shall call it 'one  $\pi^0$  image'. In this case images can be slightly wider but still might imitate interesting us primaries. However the main axis orientation of a false  $\gamma$  or a one  $\pi^0$  image is random in opposite to real  $\gamma$  events where main axis is directed towards the centre of the camera (if the telescope is directed towards a  $\gamma$ -ray source). A false  $\gamma$  or one  $\pi^0$  image can happen more likely for a low energy primary hadron than for one with higher energy.

In this article the fraction of the false  $\gamma$  events in the proton showers is calculated from the Monte Carlo simulations for the MAGIC telescope. In the following I present a MC study, discuss the similarity of the false and real  $\gamma$  image parameters.

## 2 Experiment

The MAGIC telescope [8] started to operate at the end of 2003. It is situated in the Canary Island of La Palma (28.8N, 17.9W) at the Roque de los Muchachos Observatory, 2200 m above sea level. Currently it is the largest working IACT in the world. The telescope frame made by carbon fiber tubes, has a parabolical shape with the focal length 17 m. The diameter of the telescope is 17m. The main dish is covered by more than 900  $0.5 \times 0.5 \text{ m}^2$  aluminium mirrors to achieve a final telescope area  $234\text{m}^2$ . The inner part of the camera consists of 397 photomultipliers (ET 9116) with diameter  $0.1^\circ$ . The additional 180 PMT (ET9117) with diameter  $0.2^\circ$  are outer part of the camera. The hexagonal shape camera covers in total  $4^\circ$ . There are 325 pixels (in the inner part) used for trigger. The trigger requires time coincidence and neighbour logic.

## 3 Monte Carlo simulations

The CORSIKA code version 6.023 [9] was used in simulations.  $5.025 \times 10^6$  proton-induced showers were simulated in the energy range 30 GeV- 1 TeV with the differential spectral index -2.75. The simulations were done for zenith angle  $20^\circ$  and azimuth  $0^\circ$  (showers directed to the north) with the cone opening angle of the shower direction  $3^\circ$ . The maximum of the impact parameter was chosen as 500 m. In  $\gamma$  cascade simulations the impact parameter is distributed up to 300 m. The direction of 35000 simulated  $\gamma$  events was fixed to zenith angle  $20^\circ$  and azimuth angle  $0^\circ$  and the energy range from is 10 GeV to 30 TeV with spectral index -2.6.

The standard CORSIKA code was modified to keep additional information about each subcascade created in the EAS. Each Cherenkov photon has determined a charge particle responsible for its creation. The simulations were done for MAGIC as an example of a stand-alone air Cherenkov telescope [8,10]. The Rayleigh and Mie scattering were taken into account according to the Sokolsky formula [11]. The full geometry of the mirrors and their imperfections were considered in a reflector program. The next step of the detector simulations included the camera properties, such as additional reflections in Winston cones, photocathode quantum efficiency [10] and its fluctuation, and the photoelectron collection efficiency.

The night sky background (NSB) was not included in the simulations because the pure physical effect seems to me more interesting. The photons from NSB have a random arrival time distribution. On the one side NSB may slightly increase the number of triggered events in both primaries proton and  $\gamma$  cases. On the other side adding NSB requires so-called cleaning procedure and by doing that on too high level one may make images artificially narrower and by that presented analyses less reliable.

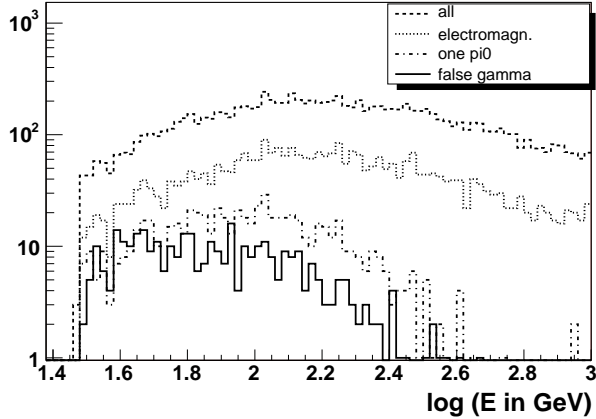


Fig. 1. The MC simulated energy distribution for trigger threshold 4 a.u..

To consider the simulated shower as a triggered event it was required that the output signals in 4 next neighbouring pixels (4 NN) exceed thresholds in time gate 3 ns. The proper discriminator simulations including arrival time of the photoelectrons and superimposed photoelectron pulses were done [12]. As trigger thresholds four possibilities were chosen: 4, 6, 8, 10 a.u., which corresponds respectively to 4, 6, 8, 10 photoelectrons coming at the same time.

## 4 Results and discussion

Proton-induced showers which images have no contributions from hadrons or muons (I called them electromagnetic images or events), are possible false  $\gamma$  and one  $\pi^0$  candidates. The simulated energy distribution of triggered events, for trigger threshold 4 a.u., is shown in Fig1. Four lines in the figure correspond to 4 cases: all triggered, electromagnetic, one  $\pi^0$  and false  $\gamma$  events respectively. Around 93% of all false  $\gamma$ 's have primary energy below 200 GeV. Primary energy of the proton is lower than 300 GeV for 97% of all one  $\pi^0$  events.

Figure 2 shows the impact parameter distributions of triggered proton events. The electromagnetic images (dotted histogram in the graph) occur more seldom for impact smaller than 90 m because Cherenkov photons produced by hadrons and muons are expected for these distances from the core axis. The distributions for false  $\gamma$  and one  $\pi^0$  are almost flat for impacts larger than 90 m. The distribution of the angular distance between the telescope and shower axes (and in the figures it is call OFF) is presented in Fig.3. It is seen that there are no favourite inclination angles for finding false  $\gamma$  or one  $\pi^0$  events in the simulated view cone.

The distribution of the number of subcascades for electromagnetic events is shown in Fig.4. The first histogram bin presents all false gammas, one  $\pi^0$  are a

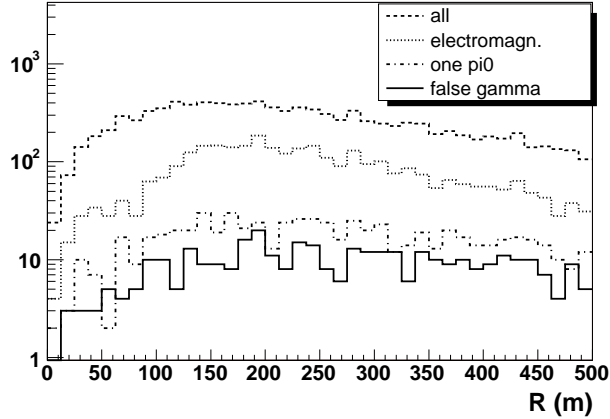


Fig. 2. The impact parameter distributions of triggered protons for trigger threshold 4 a.u..

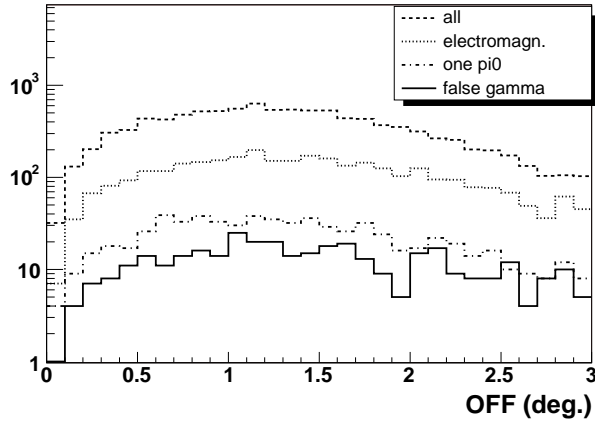


Fig. 3. The distributions of the angular distance between telescope axis and shower axis (OFF) for trigger threshold 4 a.u..

part of the second bin, the rest contains images made by 2  $\gamma$ 's from 2 different  $\pi^0$ 's.

The most interesting question is how often the protonic CR background can produce false  $\gamma$  and one  $\pi^0$  images. The dependence of this fraction on the trigger threshold is shown in Fig.5. Additionally also the electromagnetic images are plotted. The contribution of false  $\gamma$  in all triggered events is decreasing from 3.5% to 1% with increasing trigger thresholds from 4 a.u. to 10 a.u.. The estimated fraction of one  $\pi^0$  images is changing from 6.5% to 2%.

Figure 6 shows the so called size distribution. The image size is the sum of detected photoelectrons. False gammas have small sizes because their primary energy is low and they are events with quite large impact parameter. It can be seen in Fig.6 that also one  $\pi^0$  images have small sizes.

The fraction of false  $\gamma$  and one  $\pi^0$  events in the triggered proton induced

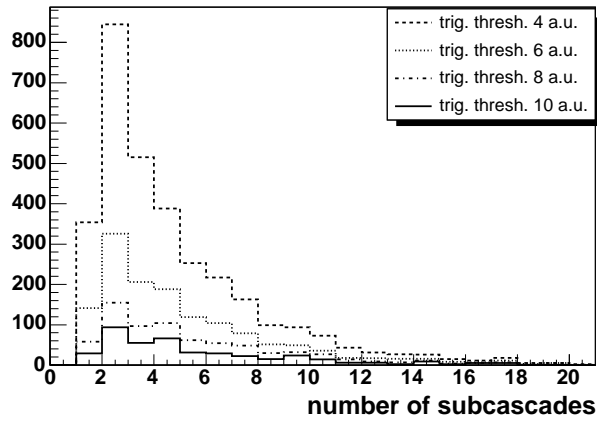


Fig. 4. The distribution of the number of subcascades contributing to the image. Events with even one Cherenkov photon produced by hadron or muon are excluded

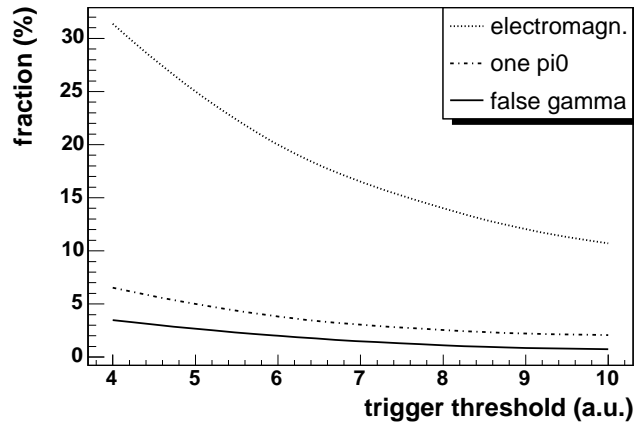


Fig. 5. The fraction of the interesting events in the total protonic background as a function of the trigger threshold.

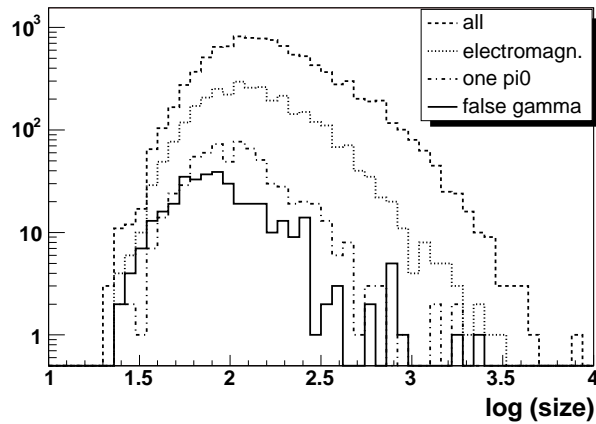


Fig. 6. The log(size) distributions for proton showers; trigger threshold 4 a.u.

Table 1

The fraction of an unrecognized by shape images in the total triggered proton events for five size bins (trigger threshold 4 a.u.).

Size (ph.e.)	false gamma (%)	one $\pi^0$ (%)	position of the energy peak (GeV) for $\gamma$ simulations
<100	8.6	11.2	30
(100,160)	2.7	8.0	50
(160,250)	1.6	4.1	70
(250,400)	1.1	3.5	100
>400	0.7	1.4	160

showers depends on the chosen size interval. Each size bin corresponds to the reconstructed energy of primary  $\gamma$ 's. One may estimate this energy as a peak position in the simulated energy distribution for the given size interval (spectral index of the simulations is -2.6). The results are summarized in Table 1. The expected background from both false  $\gamma$  and one  $\pi^0$  images is 5% for energy of real  $\gamma$  around 100 GeV and it increases significantly at lower energies.

The width is one of the Hillas parameters describing the image shape. The comparison of the width distributions of the simulated  $\gamma$ , false  $\gamma$  and one  $\pi^0$  images is presented in Fig.7. No cleaning procedure was applied to MC simulations to show the effect of shower development only. One may conclude from Fig.7 that  $\gamma$  and false  $\gamma$  or  $\pi^0$  do not differ in width distribution, so this parameter is not a good variable to distinguish real  $\gamma$ 's from protonic background. The distribution of one  $\pi^0$  events looks a little shifted (in direction of higher width) because the angular distribution of charged particles in one  $\pi^0$  events is wider than in the false  $\gamma$ 's. The directions of two gammas after  $\pi^0$  decay are not the same, but their separation angle may be smaller than one degree what is comparable with the Cherenkov light cone opening angle.

Another Hillas parameter describing the image shape is length. The length distributions of images made by real  $\gamma$ , false  $\gamma$  and one  $\pi^0$  are shown in Fig.8. In the case of real  $\gamma$ 's the distribution is slightly narrower than in the case of false  $\gamma$  and one  $\pi^0$ . One may explain this fact by a different inclination angle (OFF). Gammas were simulated parallel the to telescope axis and a smaller part of the longitudinal cascade is visible in the telescope's FOV. False  $\gamma$  and one  $\pi^0$  as a part of protonic events are inclined to the telescope axis and thus it may happen that a longer part of the shower is visible resulting in a larger image length. As it is a geometrical effect the opposite scenario is also possible; the observed longitudinal part of the shower is shorter than in real  $\gamma$  case and then false  $\gamma$  images have smaller length. The second effect is not visible in one  $\pi^0$  events because products of its decay are separated by angle.

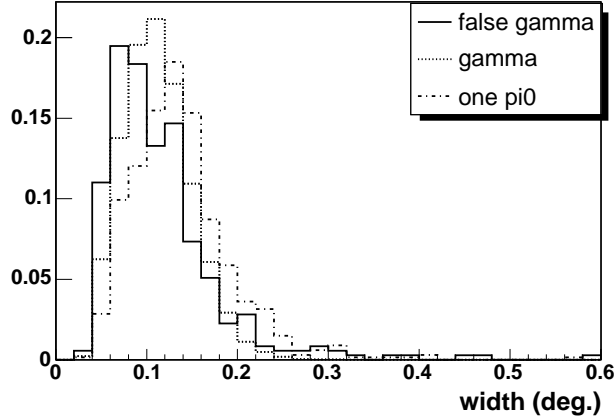


Fig. 7. The width distributions obtained in MC  $\gamma$ , false  $\gamma$  and one  $\pi^0$  events for trigger threshold 4 a.u.. Histograms are normalized to 1.

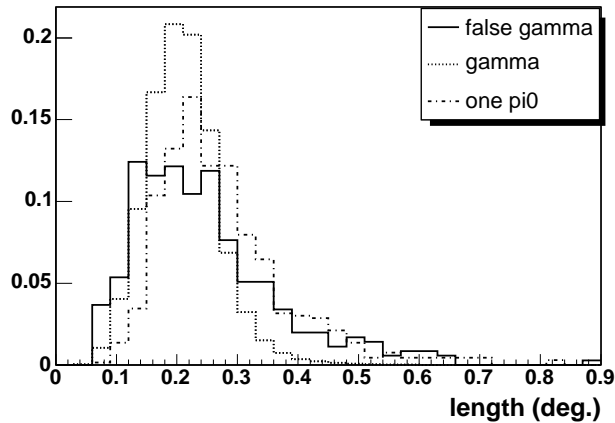


Fig. 8. The length distributions obtained in MC  $\gamma$ , false  $\gamma$  and one  $\pi^0$  events for trigger threshold 4 a.u.. Histograms are normalized to 1.

It was checked that the distributions of alpha parameter are flat for all cases: electromagnetic, one  $\pi^0$  or false  $\gamma$  image. This parameter can be still efficiently used in  $\gamma$ /hadron separation.

## 5 Conclusion

The simulations show that images produced by Cherenkov photons from one electromagnetic subcascade in proton-induced showers occur in large telescopes. 93% of such events have the primary energy of protons lower than 200 GeV in case of the MAGIC telescope for trigger thresholds from 4 a.u.. Their impact parameter is larger than 90m and there is no special dependence on the inclination angle of the shower axis to the telescope axis. The fraction of such events in the total protonic background decreases with increasing trig-

ger threshold as 3.5% to 1% for thresholds from 4 to 10 a.u. It was shown that sizes of such events are small, mostly below 400 photoelectrons. The images of these events have shapes very similar those from primary  $\gamma$ 's and their width distributions are almost exactly the same. There is a difference between length distributions caused by different shower direction distributions. It was also presented that images from two subcascades from the same  $\pi^0$  appear in the trigger. Their fraction is estimated from 6.5% to 2% for trigger thresholds from 4 to 10 a.u. The images are only a little wider and longer than  $\gamma$  images so real  $\gamma$  separation from them is not possible by using shape parameters only. In the low energy below 100 GeV,  $\gamma$ /hadron separation is much more difficult due to existence possible unwanted false  $\gamma$  and one  $\pi^0$  background. We may expect such background to be flat in the alpha plot (even after first procedure of the  $\gamma$  candidates selection) for small image sizes. In the experiment the final background is estimated from the fit in the alpha plot, but the efficiency of  $\gamma$ /hadron separation will decrease at low energies due to the presented natural limit.

### Acknowledgements

This work was supported by Polish KBN grant No. 1P03D01028.

### References

- [1] Weekes T. C. et al., ApJ, 342, (1989)
- [2] Hillas A. M., 19th ICRC, La Jolla, 3, 445 (1985)
- [3] Mori M. et al., CANGAROO-III: Status Report, in B. Degrang and G. Fontaine (eds.), Proc. Towards a Network of Atmospheric Cherenkov Detectors VII Conf., Ecole Polytechnique, Palaiseau, France, 27-29 April 2005, pp. 19-27
- [4] Hofmann D. et al., H.E.S.S. Status, in B. Degrang and G. Fontaine (eds.), Proc. Towards a Network of Atmospheric Cherenkov Detectors VII Conf., Ecole Polytechnique, Palaiseau, France, 27-29 April 2005, pp. 43-56
- [5] Mariotti M. et al., MAGIC: Status Report, in B. Degrang and G. Fontaine (eds.), Proc. Towards a Network of Atmospheric Cherenkov Detectors VII Conf., Ecole Polytechnique, Palaiseau, France, 27-29 April 2005, pp. 29-41
- [6] Weekes T.C. et al., VERITAS: History and Status, in B. Degrang and G. Fontaine (eds.), Proc. Towards a Network of Atmospheric Cherenkov Detectors VII Conf., Ecole Polytechnique, Palaiseau, France, 27-29 April 2005, pp. 3-17
- [7] Mirzoyan R. et al. Astropart. Phys. 25, 342, (2006)
- [8] Albert J. et al. Astropart. Phys. 23, 493, (2005)
- [9] Knapp J., Heck D., EAS Simulation with CORSIKA: A Users Manual, 2004

- [10] Barrio J. A. et al., The MAGIC Telescope Design Study, Munich, (1998)
- [11] Sokolsky P., "Introduction to Ultrahigh Energy Cosmic Ray Physics", Addison-Wesley.,(1989)
- [12] Sobczyńska D., Lorenz E., Nucl. Instrum. Methods Phys. Res. A 490, 124, (2002)